

1 Beyond accuracy : score calibration in deep learning models
2 for camera trap image sequences

3 Gaspard Dussert¹, Simon Chamaillé-Jammes^{*2}, Stéphane Dray¹ and Vincent
4 Miele¹

5 ¹Université Lyon 1, CNRS, UMR 5558, Laboratoire de Biométrie et Biologie
6 Evolutive, Villeurbanne, France

7 ²CEFE, Université de Montpellier, CNRS, EPHE, IRD, Montpellier, France

8 November 9, 2023

9 **Abstract**

10 1. In this paper, we investigate whether deep learning models for species classi-
11 fication in camera trap images are well calibrated, i.e. whether predicted confidence
12 scores can be reliably interpreted as probabilities that the predictions are true. Ad-
13 ditionally, as camera traps are often configured to take multiple photos of the same
14 event, we also explore the calibration of predictions at the sequence level.

15 2. Here, we (i) train deep learning models on a large and diverse European
16 camera trap dataset, using five established architectures; (ii) compare their calibra-
17 tion and classification performances on three independent test sets; (iii) measure the
18 performances at sequence level using four approaches to aggregate individuals pre-
19 dictions; (iv) study the effect and the practicality of a post-hoc calibration method,
20 for both image and sequence levels.

*simon.chamaillé@cefe.cnrs.fr

21 3. Our results first suggest that calibration and accuracy are closely intertwined
22 and vary greatly across model architectures. Secondly, we observe that averaging the
23 logits over the sequence before applying softmax normalization emerges as the most
24 effective method for achieving both good calibration and accuracy at the sequence
25 level. Finally, temperature scaling can be a practical solution to further improve
26 calibration, given the generalizability of the optimum temperature across datasets.

27 4. We conclude that, with adequate methodology, deep learning models for
28 species classification can be very well calibrated. This considerably improves the
29 interpretability of the confidence scores and their usability in ecological downstream
30 tasks.

31 **Keywords** : calibration, camera trap, classification, confidence score, event, machine
32 learning

33 **1 Introduction**

34 Camera traps have become a central tool in the monitoring and conservation of com-
35 munities and populations. They generate a lot of data that can be used to infer, for
36 instance, species richness, occupancy or activity patterns (Sollmann 2018). To exploit
37 these data, it is first required to identify the species present in the photos or videos.
38 This manual annotation task is generally long and tedious, but it has been shown in re-
39 cent years that it can be replaced by an automatic classification made by deep learning
40 models, often with an accuracy of over 90% (Norouzzadeh et al. 2018; Willi et al. 2019;
41 Whytock, Świeżewski, et al. 2021).

42 Accuracy may not be the only model performance metrics to care about though.
43 Accuracy is calculated from, for each image, the prediction that has the highest confi-
44 dence score (i.e. the top-1 prediction). In many ecological studies, downstream tasks
45 may however directly rely on the confidence score of the predictions. This can be the
46 case for instance when considering that values above a certain threshold indicate true

47 detections, or when propagating model uncertainty into subsequent statistical models.

48 Importantly, confidence scores are frequently interpreted as probabilities of the pre-
49 diction being true, but this is not always the case as many models may provide biased
50 confidence scores (Gawlikowski et al. 2023). In the context of classification models, a
51 model returning confidence scores that can be reliably interpreted as probabilities of
52 the prediction being true is said to be well calibrated. For instance, if a model pre-
53 dicts the label of 100 images with a confidence score of 0.8, we would expect to observe
54 an actual accuracy of 80% on these images. However, deep learning models trained
55 with the categorical crossentropy loss, a common practice, are often over-confident and
56 poorly calibrated (Gawlikowski et al. 2023). Attention should therefore also be given
57 to the properties of confidence scores, as seen in other disciplines. For instance, good
58 calibration of deep learning models has been shown to be important for safety-critical
59 applications such as autonomous driving (Bojarski et al. 2016) or medical diagnosis
60 (Nair et al. 2018). In the field of ecology, a good calibration ease the interpretation of
61 the scores, but could also be critical if the scores are used in downstream tasks such as
62 occupancy estimation (Gimenez et al. 2022), inference of species interaction (Parsons et
63 al. 2022), real-time alert to guide law-enforcement (Whytock, Suijten, et al. 2023), and
64 confidence-score-based prediction checking on citizen science platforms (e.g. Zooniverse
65 (Simpson et al. 2014)).

66 Here we explore the calibration of confidence scores in the context of species classi-
67 fication models for camera trap data. In that context, the recurring leading approach,
68 as assessed in recent iWildcam competitions (Beery, Agarwal, et al. 2021), consists in
69 two steps: (step 1) detecting animals, humans and vehicles and filtering out empty im-
70 ages using a robust detection model such as MegaDetector (Beery, Morris, et al. 2019;
71 Mitterwallner et al. 2023) and (step 2) using a CNN classification model to identify the
72 species in the bounding box returned by the detection model, when an animal has been
73 detected. We therefore focus on these species classification models (step 2), which are de-

74 veloped for a large range of species all over the world. We explore the interplay between
75 accuracy and calibration for different state-of-the-art model architectures, using camera
76 trap data from different sources. Also, we consider the calibration of confidence scores
77 at the level of sequences of images. Indeed, camera traps are often configured to take
78 multiple photos at each trigger, and predictions aggregated at the level of the sequence
79 of images (sometimes called 'the observation' or 'event'). The issue of the calibration
80 of confidence scores at the level of sequences of images has not, to our knowledge, been
81 addressed in the literature. Furthermore, we study the relevance of a popular post-hoc
82 calibration method called temperature scaling (Platt 2000), for both image and sequence
83 levels. Finally, we provide a set of good practices for researchers and practitioners in the
84 field.

85 **2 Material and Methods**

86 **2.1 The DeepFaune Dataset**

87 We use the dataset of the DeepFaune initiative (Rigoudy et al. 2023), which is a collab-
88 orative effort involving over 50 partners who, together, have gathered over two millions
89 images and twenty thousand videos that they had manually annotated. These partners
90 are affiliated to a wide range of institutions, such as organizations managing protected ar-
91 eas, hunting federations, and academic research groups. Images and videos were mainly
92 collected in France, but also in a few European countries. Most of the annotation were
93 at the species level, but some were at a higher taxonomic level (e.g. mustelid). Videos
94 were converted into images by extracting frames of the first four seconds, with a time
95 step of one second. The dataset provides a great diversity of habitats, elevations and
96 weather conditions, as well as a wide variety of camera trap models with different set-
97 tings, resolutions, flash type and image processing.

98 **2.2 Training and validation datasets**

99 For the species classification task, it is now known (Beery, Morris, et al. 2019; Norman
100 et al. 2023) that two-step approaches (object detector followed by a classifier) are more
101 efficient than classifiers that process the whole image. We use MegaDetector v5 (MdV5)
102 (Beery, Morris, et al. 2019) to extract bounding boxes of animals, human and vehicles.
103 Because MdV5 has already near-perfect accuracy on human and vehicles we only kept,
104 for the training of our classifier, the bounding boxes that predicted the presence of an
105 animal. For each bounding box, we created a cropped image of the original image,
106 resulting in 429 347 cropped images of 22 different classes (the distribution of the classes
107 is shown in Supporting Information Figure 1).

108 To avoid overfitting and shortcut learning between the background of the images
109 (i.e. camera trap site) and the observed species, we designed the training and validation
110 sets to have disjoint pairs of background and species while having the same balance of
111 species and diversity of habitats. The validation set represented about 20% of the images
112 available while being disjoint from the training set at the species level: for each species,
113 the validation set is made of images originating from partners different than the ones
114 used in the training set, while being as close as possible to a 80/20 split. This requires
115 solving a problem of combinatorial optimization known as *subset sum problem*, which
116 is a special case of the *knapsack problem* and which can be achieved using dedicated
117 libraries (e.g. *mknapsack*). Ultimately, we had 368 786 images in the training set and
118 60 561 in the validation set.

119 **2.3 Out-of-sample test sets**

120 To demonstrate that the results of the classifier could generalize beyond the images
121 collected in the DeepFaune initiative, 3 out-of-sample test datasets were used. These
122 datasets originated from ecological programs conducted in three geographically distinct
123 areas. We refer to these datasets by the name of the areas they originate from:

124 • **Pyrenees** : camera trap study in the national reserve of Orlu in the French
125 Pyrenees, conducted by the French Biodiversity Agency (OFB), 100 266 images
126 and 12 species after preprocessing.

127 • **Alps** : camera trap study in the Ecrins national park in the French Alps, conducted
128 by S. Chamaille-Jammes, 8 106 images and 12 species after preprocessing.

129 • **Portugal** : camera trap study in the Peneda-Gerês National Park in Portugal
130 (Zuleger et al. 2023), publicly available. 99 750 cropped images and 16 species
131 after processing.

132 **2.4 Sequences of images**

133 It is common to configure camera traps to take a series of images after each trigger. It is
134 therefore relevant to have a single prediction for the whole series of images. We thereafter
135 name such series 'sequences'. In our test sets, we considered that two consecutive images
136 taken within 10s, at the same site (i.e. the same camera trap), belonged to the same
137 sequence. We obtained sequences of 1 to 213 images.

138 **2.5 Confidence score at sequence level**

139 A sequence with S images has S individual predictions that can be aggregated in many
140 different ways to produce a single prediction for the whole sequence. Formally, for a
141 sequence of S images x_i , the model predicts the logits $z_i = (z_{i1}, \dots, z_{iK})$ for each image,
142 with K the number of classes. Confidence scores are derived using the softmax function
143 : $p_i = (p_{i1}, \dots, p_{iK}) = \text{softmax}(z_{i1}, \dots, z_{iK})$. We aimed at predicting the confidence scores
144 of the sequence $p_{seq} = (p_{seq1}, \dots, p_{seqK})$ as a function of the predictions at the image
145 level. We explored four different aggregation functions:

146 • **Average Score** : We averaged, over the sequence, the scores for individual pic-

147 tures of the sequence:

$$p_{seq} = \left(\frac{1}{S} \sum_{i=1}^S p_{i1}, \dots, \frac{1}{S} \sum_{i=1}^S p_{iK} \right) \quad (1)$$

148 • **Average Logit** : We averaged, over the sequence, the logits for individual pictures
149 of the sequence, and then applied the softmax function:

$$p_{seq} = \text{softmax} \left(\frac{1}{S} \sum_{i=1}^S z_{i1}, \dots, \frac{1}{S} \sum_{i=1}^S z_{iK} \right) \quad (2)$$

150 • **Max Score** : We kept the scores of the image that had the highest score amongst
151 all scores of all images of the sequence:

$$p_{seq} = p_{i^*}, \text{ with } i^* = \arg \max_{i \in [1, S]} \left\{ \max_{k \in [1, K]} \{p_{ik}\} \right\} \quad (3)$$

152 • **Max Logit** : We kept the scores of the image that had the highest logit amongst
153 all logits of all images of the sequence:

$$p_{seq} = p_{i^*}, \text{ with } i^* = \arg \max_{i \in [1, S]} \left\{ \max_{k \in [1, K]} \{z_{ik}\} \right\} \quad (4)$$

154 2.6 Calibration metrics

155 For a set of N images, we define the true class of the i -th image y_i and $p_i = (p_{i1}, \dots, p_{iK})$
156 the confidences scores of the K classes. The predicted class \hat{y}_i is the top-1 classification
157 prediction, that is the class with the greatest confidence score, denoted s_i :

$$\hat{y}_i = \arg \max_{k \in [1, K]} p_{ik} \quad \text{and} \quad s_i = \max_{k \in [1, K]} p_{ik} \quad (5)$$

158 For M evenly spaced bins, we can define b_m the set of indices i such as $s_i \in]\frac{m-1}{M}, \frac{m}{M}]$

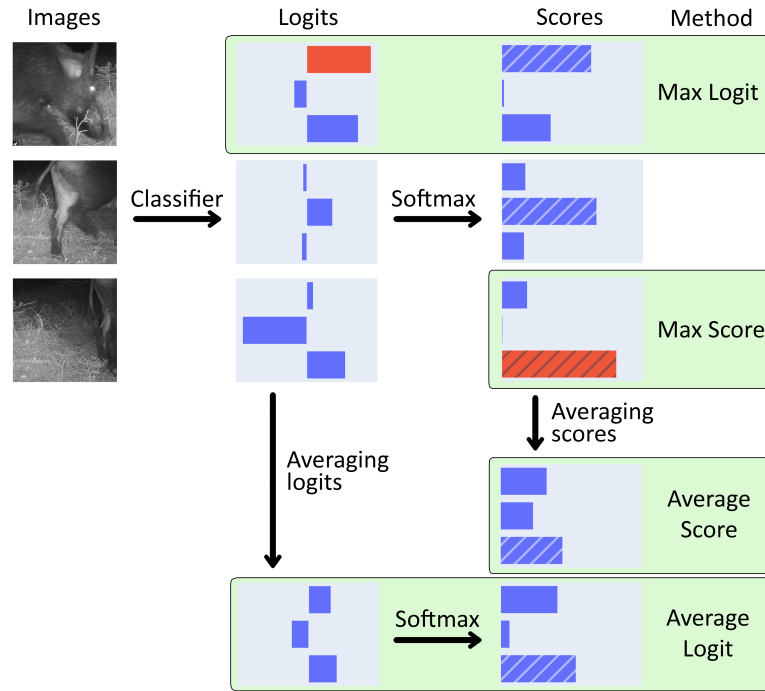


Figure 1: Illustration of the four aggregation methods. The greatest overall logit and score are in red. The top-1 score is hatched to emphasize that only this score is used to calculate the calibration.

159 and compute the average bin accuracy and the average bin confidence score :

$$\text{acc}(b_m) = \frac{1}{|b_m|} \sum_{i \in b_m} \mathbb{1}(\hat{y}_i = y_i) \quad (6)$$

160

$$\text{conf}(b_m) = \frac{1}{|b_m|} \sum_{i \in b_m} s_i \quad (7)$$

161 The bin-wise accuracy can be plotted to construct the reliability histogram (Guo et
 162 al. 2017) (e.g. Supporting Information Figure 3). It allows to visualize the calibration of
 163 a model: the closest the tops of the histogram bars are from the identity line, the better
 164 calibrated the model is. In addition, if the tops of the histogram bars are mostly above
 165 (resp. below) the line, the model is said to be under-confident (resp. over-confident).

166 The most common metric to measure the model's calibration quantitatively is the

167 Expected Calibration Error (ECE) (Guo et al. 2017). ECE is defined as the bin-wise
168 calibration error weighted by the size of the bin :

$$\text{ECE} = \sum_{m=1}^M \frac{|b_m|}{N} |\text{acc}(b_m) - \text{conf}(b_m)| \quad (8)$$

169 Due to the large amount of images in our test sets, we decided to use a greater number
170 of bins, specifically 20 instead of the standard 15, to obtain a more precise measurement
171 of calibration with the ECE. In addition to this metric, we evaluated the classification
172 performance of our classifier with the accuracy metric. These two metrics can also be
173 used to evaluate the classification and the calibration at the sequence level, using the
174 score p_{seq} and the associated predicted label $\hat{y}_{seq} = \arg \max_{k \in [1, K]} p_{seq}$.

175 2.7 Temperature Scaling

176 Temperature scaling (Platt 2000) is a post-processing method to improve the calibration
177 of the model after the training. The scores predicted by the model are rescaled by a
178 temperature parameter $T > 0$ using a generalization of the softmax function :

$$p_{ij} = \frac{\exp^{z_{ij}/T}}{\sum_{k=1}^K \exp^{z_{ik}/T}} \quad (9)$$

179 For $T = 1$ the scores obtained are the same as with the standard softmax function.
180 $T > 1$ leads to lower scores and helps when the model is over-confident. Conversely,
181 $T < 1$ increases the scores and helps under-confident models. For a given dataset, it is
182 possible to determine the optimal temperature T^* , that minimize the ECE. However,
183 this optimum temperature may differ from one dataset to another, and determining the
184 optimum requires access to the labels. It is therefore unrealistic to use this individ-
185 ual temperature T^* to compare methods, as it cannot be calculated for a new dataset
186 without manually annotating a fraction of the data. Instead, we propose to look at
187 performance using a single temperature \bar{T} shared across the three datasets. We define

188 \bar{T} as the temperature that minimizes the average ECE across the 3 test datasets. Tem-
189 perature scaling can be combined with the four aggregation method (Section 2.5) to
190 calibrate sequence level predictions by simply replacing the standard softmax function
191 with Equation 9.

192 **2.8 Deep learning models**

193 We used 5 established machine learning architectures: EfficientNetV2, ConvNext, ViT,
194 Swin Transformer V2, and MobileNetV3. (Tan and Le 2021; Zhuang Liu et al. 2022;
195 Dosovitskiy et al. 2021; Ze Liu et al. 2022; Howard et al. 2019). We have selected these
196 architectures to represent CNNs (EfficientNetV2, ConvNext), Transformers (Swin, ViT),
197 as well as lightweight architectures that could be deployed in camera traps that do the
198 classification at the edge (MobileNetV3). Models were trained using the TIMM library
199 (Wightman 2019) with transfer-learning from ImageNet-22k (Ridnik et al. 2021), the
200 largest publicly available database. Data augmentation was applied using the imgaug
201 library (A. B. Jung et al. 2020) using only standard transformations such as flips, crops,
202 conversion to grayscale and affine transformation. The optimization was done using
203 SGD, with a batch size of 32 and a different learning rate adapted for each architecture.
204 To avoid overfitting, early stopping was used while monitoring the validation accuracy
205 and with a patience of 10 epochs.

206 **3 Results**

207 **3.1 Calibration at the image level**

208 Generally, we observed that calibration (as measured by ECE) was negatively correlated
209 with accuracy across models, for the 3 test datasets (Figure 2). ConvNext was the model
210 providing the best overall performance. In particular, this model was slightly better in
211 accuracy but much more efficient in terms of calibration (ECE of 2.37%, more than

212 2 times less than the second-best model, Swin Transformer V2, which has an ECE of
 213 5.04%) on the Portugal dataset. In the meantime, the lightweight model, MobileNet,
 214 had bad to very bad (ECE of 34.27% on the Portugal dataset) accuracy and calibration
 215 performances.

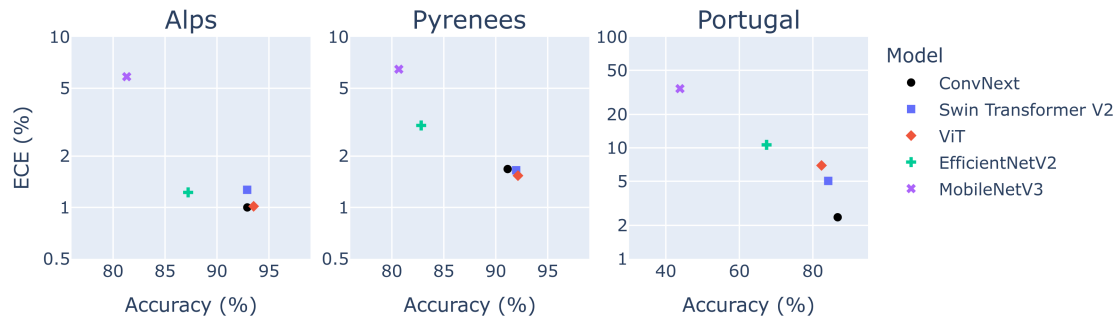


Figure 2: Scatterplot of ECE vs. accuracy values for five models (colored points) and three test data sets (panels), computed at the image level. Here, the ECE is not post-calibrated with temperature scaling (i.e. the temperature is 1 for all models).

216 As expected, temperature scaling allowed improving ECE values, for all models and
 217 datasets. We almost always observed a V-shape relationship between ECE and tem-
 218 perature, with ECE increasing quickly and by several percents around the optimum
 219 temperature value (Figure 3). This optimum temperature was generally greater than
 220 1, suggesting that all models were initially overconfident to a greater or lesser extent.
 221 Interestingly, the V-shape curves of the different datasets overlapped well for the most
 222 accurate models (ConvNext and transformed-based models, ViT and Swin), and opti-
 223 mum temperature were similar across datasets. This suggested that a single optimum
 224 temperature would be sufficient to achieve efficient post-processing calibration. Indeed,
 225 using temperature scaling with temperature \bar{T} , the models exhibited on average a rela-
 226 tive reduction in ECE of 38% compared to without temperature scaling ($T = 1$) (dashed
 227 line in Figure 3).

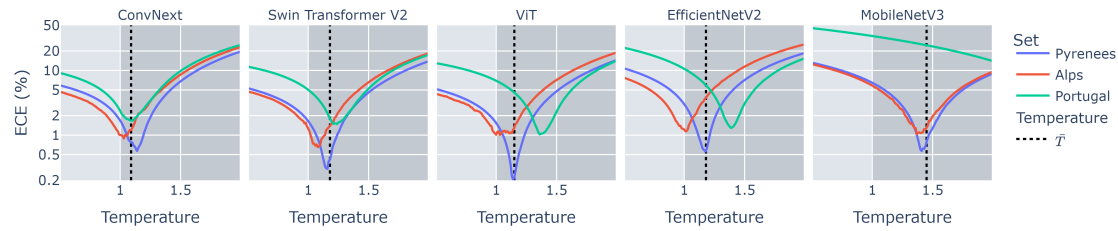


Figure 3: Curves of ECE values along the gradient of temperature values, for five models (panels) and three test data sets (colored curves). An optimum temperature below 1 indicates an underconfident model (light gray area), and above 1 indicates an overconfident model (dark gray area). The vertical dashed line shows \bar{T} , the temperature that minimized the average ECE across the 3 test datasets.

228 3.2 Calibration at the sequence level

229 Classification accuracy was much greater at the sequence level than at the image level
230 (Figure 4 top). This was true for all models and all datasets, with up to +10% of
231 accuracy for MobileNetV3 on the Portugal dataset. The Average Score and Average
232 Logit were the two best methods for maximizing accuracy, with a slight advantage for
233 the former. The gain in accuracy was however lower for models that were already
234 efficient at the image level (ConvNext, ViT and SwinTransformer), but those remained
235 the best models at the sequence level. Importantly, of the two aggregation methods
236 that improved accuracy most, Average Score and Average Logit, only Average Logit
237 provided well calibrated scores (Figure 4 bottom). The Average score was actually the
238 worst aggregation method for calibration. Therefore, considering both accuracy and
239 calibration metrics, the Average Logit was the best aggregation method.

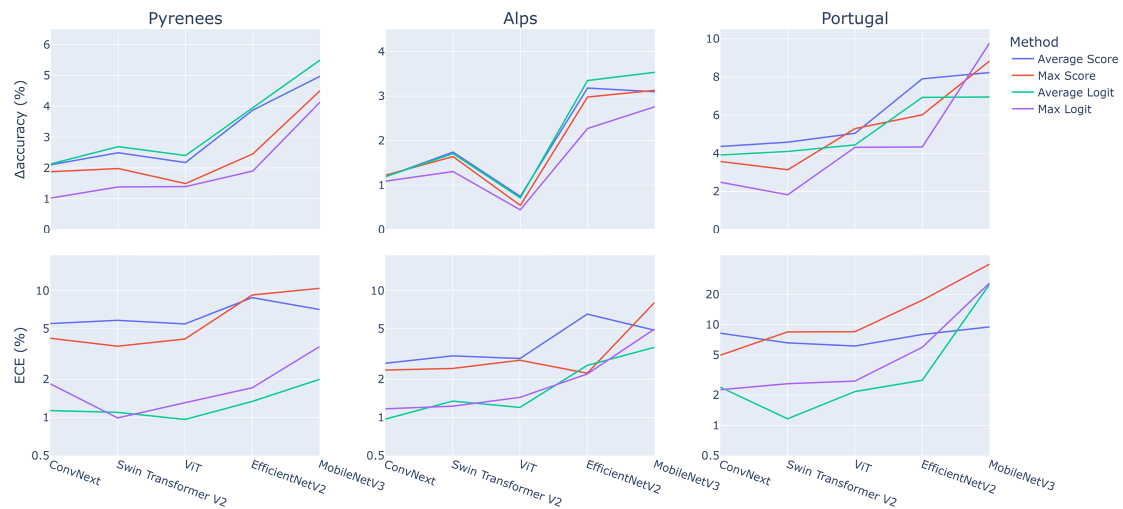


Figure 4: Δ Accuracy (top, the greater the better) and ECE (bottom, the lower the better) for the four aggregation methods (colored curves) and five models (x-axis) on three test data sets (3 panels). Δ Accuracy is the difference between the accuracy at the sequence level and the accuracy at the image level.

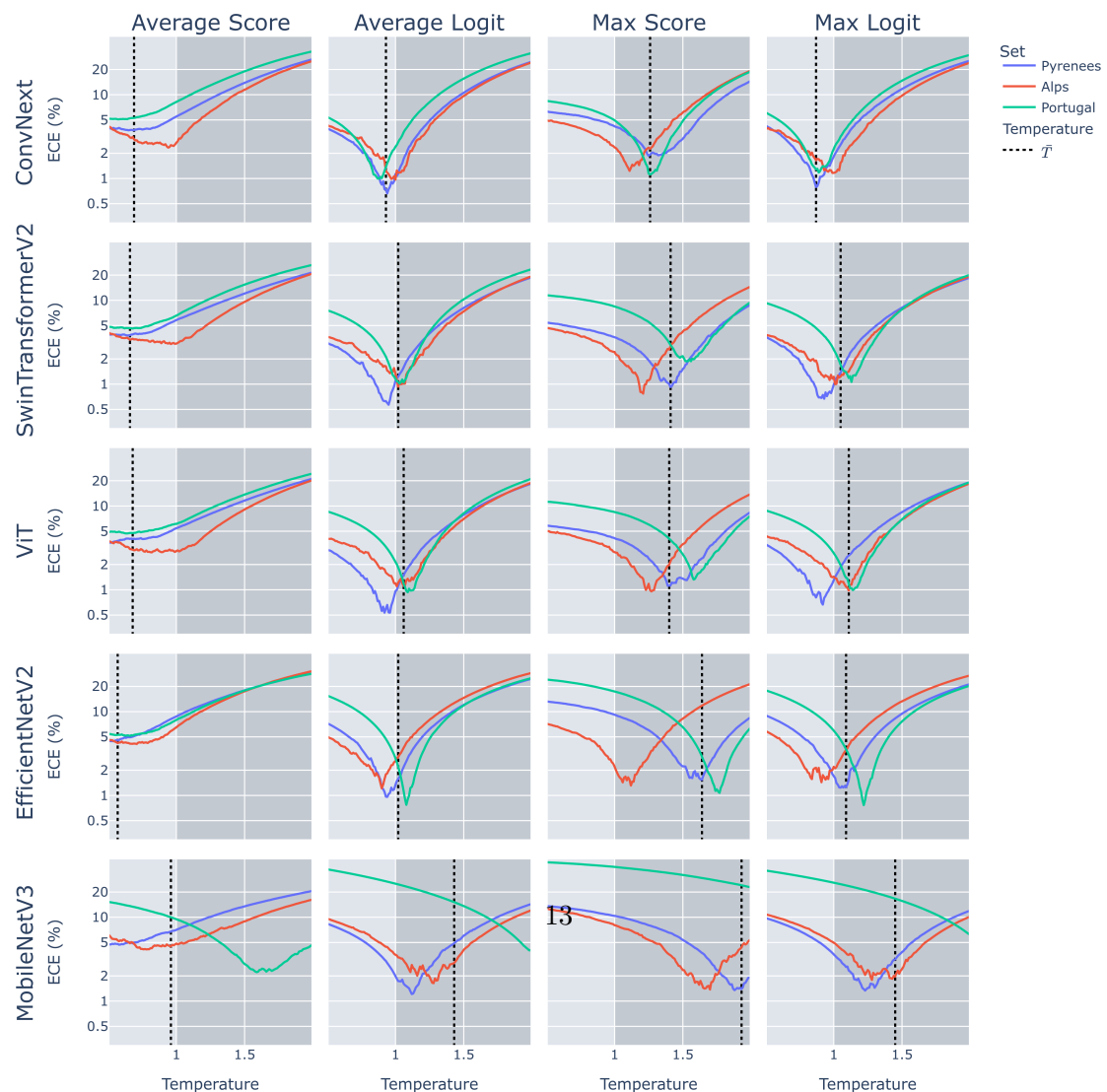


Figure 5: Curves of ECE values along the gradient of temperature values, for the four aggregation methods (columns), the five models (rows) and the three test datasets (colored curves). Light/gray area and dashed line defined as in Figure 3.

240 We finally studied the interplay between temperature scaling and aggregation meth-
241 ods. We observed that the aforementioned V-shape was more flat for the Average Score
242 method than for the other methods (first column in Figure 5 versus the others). This
243 confirmed that this method was the worst method, even with temperature scaling. We
244 also noted that the Average Logit method provided the lowest ECE values overall (1.17%
245 on average), and thus remained the best method, with temperature scaling further im-
246 proving calibration at sequence level.

247 Looking at \bar{T} and the optimum temperature of each set (minima and dashed lines
248 on Figure 5), it can be noted that using the Average Score methods led models towards
249 underconfidence, whereas using the Max Score methods led them towards overconfidence.
250 This observation is also visible in the reliability histogram, as shown in Supporting
251 Information (Supplementary Figure 3). Meanwhile, models using the Average Logit
252 method displayed optimum temperatures close to 1 and, as a consequence, a temperature
253 \bar{T} close to 1 as well. We therefore concluded that the Average Logit method did not
254 led to under- or over-confidence of models in our experiments. Also, and as observed at
255 the image level, a single temperature (possibly close to 1) would be sufficient to achieve
256 good post-processing calibration with the Average Logit method.

257 4 Discussion

258 This study assessed the calibration of confidence scores, at image and sequence level, for
259 different deep learning models in the context of species classification in camera trap data.
260 Using five state-of-the-art models and three out-of-sample test datasets, we showed that
261 score calibration can vary greatly across model architectures, in a way that is consistent
262 across test sets. Further, we showed that the different aggregation methods to obtain
263 scores at the sequence level gave very different calibration values, and that the Average
264 Logit method must be preferred over the others for optimizing both accuracy and cal-

265 ibration. Finally, we showed that temperature scaling can be used both at image level
266 and sequence level, with a single temperature \bar{T} that do not have to vary across datasets,
267 to further improve the calibration. These observations pave the way for practitioners
268 that are invited to 1/ monitor calibration as well as accuracy, 2/ use the Average Logit
269 method and 3/ estimate the optimal temperature on their own test dataset and use it
270 for the model deployment.

271 Differences in models' performance can be partly explained by model size. Indeed we
272 found that models with the highest number of parameters (ConvNext, ViT, SwinTrans-
273 former) gave the best accuracy and ECE values. On the other hand, the only lightweight
274 model, MobileNet, was consistently the worst model. Despite some literature showing
275 that neural networks can be poorly calibrated, our result shows that this is not always the
276 case (see also Minderer et al. (2021)), and that certain families of model architectures,
277 such as ConvNext here, are intrinsically better calibrated than others, independently of
278 the size of the model. The calibration of each model can be further improved on each
279 dataset using temperature scaling as post-processing function. However, determining
280 the optimal T requires annotating at least a fraction of the target set of images, which
281 is something that practitioners would like to avoid if possible. Fortunately, we showed
282 empirically with three very different datasets that the optimal temperatures are very
283 close from one dataset to another, which suggests the generalizability of a single temper-
284 ature that can be determined and fixed for future test sets. That said, we do not claim
285 that the optimal temperatures defined in this paper can be used directly when using one
286 of the studied architectures. Indeed, these temperatures are valid for a given training
287 procedure (datasets, hyperparameters). In practice, it is mandatory to estimate the
288 temperature using available test dataset(s) and subsequently maintain this temperature
289 for deployment (since we showed it will be generalizable). This way, when the model will
290 be used to classify new unseen data, the previously estimated temperature will ensure a
291 better calibration of the predicted scores.

292 Proper model calibration at the image level is not always sufficient, as many soft-
293 ware programs and scientific studies operate at the scale of the sequences that define
294 the relevant 'observations' or 'events' from an ecological viewpoint. It is therefore ex-
295 tremely important to be able to calibrate the predictions at sequence level. For the first
296 time, we showed that the most intuitive approach, in which scores are averaged, did not
297 provide the best accuracy and had the worst calibration, with largely under-confident
298 predictions. Interestingly, our findings can be confirmed by the analogy with ensemble
299 models. These approaches use N models to make a prediction on *one* image, whereas we
300 use N images to make a prediction with *one* model at the sequence level. Wu and Gales
301 (2021) showed that for ensemble models, individual model calibration is not sufficient to
302 yield a calibrated ensemble prediction, and that their own method, which is equivalent to
303 Average Score approach also leads to under-confidence. Moreover, Rahaman and Thiery
304 (2021) show that, thanks to this natural shift in the optimal temperature when models
305 are ensembled, if the individual models were slightly overconfident ($T > 1$, as is often the
306 case in deep learning) then the ensemble model was naturally calibrated ($T \sim 1$). Our
307 results greatly support the use of the Average Logit method for aggregating individual
308 scores at the sequence level. It shifts slightly the optimal temperature towards undercon-
309 fidence, which counterbalanced the overconfident nature of deep learning networks, and
310 resulted in sequence level prediction that are almost calibrated without post-processing.
311 With Average Logit, it is still interesting to use temperature scaling to improve calibra-
312 tion as much as possible, especially given that the ECE minima are again very close to
313 each other and allow a single temperature to be set.

314 In this work, we focused on temperature scaling and did not consider other methods
315 that have been shown to sometimes improve calibration, such as label smoothing and
316 mixup (Szegedy et al. 2015; Zhang et al. 2018). We did so because these two methods
317 are actually debated, as several studies have showed that they can actually worsen cal-
318 ibration when combined with temperature scaling (Wang et al. 2023; Minderer et al.

319 2021). As Minderer et al. (2021) state, "label smoothing creates artificially underconfi-
320 dent models and may therefore improve calibration for a specific amount of distribution
321 shift". Label smoothing also assumes that all incorrect classes are equally likely (Maher
322 and Kull 2021), which is obviously problematic in ecology (e.g., a wrongly predicted
323 roe deer is much more likely to be a red deer than a wolf). Mixup also deteriorates
324 calibration properties of networks by creating non-realistic images in the training set
325 and leading to substantial distributional shift (Rahaman and Thiery 2021; Gawlikowski
326 et al. 2023).

327 We believe that our results could be of use to researchers and practitioners in the
328 field of computer vision of camera trap images. Firstly, we encourage everyone to select
329 the architecture of their model using not only accuracy but also by calculating the ECE.
330 Secondly, we recommend using the Average Logit method to aggregate information at
331 sequence level, as it performs very well in terms of accuracy and calibration. Finally,
332 to use temperature scaling and make calibration even better, the optimum temperature
333 can be calculated on a test dataset and kept for future datasets.

334 **Acknowledgements**

335 This work was granted access to the HPC resources of IDRIS under the allocation 2022-
336 AD010113729 made by GENCI.

337 We acknowledge the organizations and people contributing to the DeepFaune initiative.

338 **Conflict of interest**

339 None of the authors has a conflict of interest.

340 **Author contributions**

341 G.D., S.C.J., S.D. and V.M. conceived the ideas and designed the methodology. G.D.,
342 S.C.J. and V.M. gathered the training data. S.C.J collected the data of the Alps test
343 set. G.D. and V.M. coded and performed the analysis. G.D. wrote the first version of
344 the manuscript, S.C.J., S.D. and V.M. contributed critically to the drafts and gave final
345 approval for publication.

346 **Data availability statement**

347 The five trained models, all derived data used in the analysis, and the code for the infer-
348 ence and metric calculation are available at <https://doi.org/10.5281/zenodo.10014376>.
349 The Portugal and Alps datasets are available at <https://doi.org/10.15468/rah33j> and
350 <https://doi.org/10.5281/zenodo.10014376>. The Pyrenees dataset is available upon re-
351 quest only, because of the presence of a sensitive species (brown bear).

352 **References**

- 353 Beery, Sara, Arushi Agarwal, Elijah Cole, and Vighnesh Birodkar (2021). *The iwildcam*
354 *2021 competition dataset*. arXiv:2105.03494 [cs].
- 355 Beery, Sara, Dan Morris, and Siyu Yang (July 2019). *Efficient Pipeline for Camera Trap*
356 *Image Review*. arXiv:1907.06772 [cs]. DOI: 10.48550/arXiv.1907.06772.
- 357 Bojarski, Mariusz, Davide Del Testa, Daniel Dworakowski, Bernhard Firner, Beat Flepp,
358 Prasoon Goyal, Lawrence D. Jackel, Mathew Monfort, Urs Muller, Jiakai Zhang, Xin
359 Zhang, Jake Zhao, and Karol Zieba (Apr. 2016). *End to End Learning for Self-Driving*
360 *Cars*. arXiv:1604.07316 [cs]. DOI: 10.48550/arXiv.1604.07316.
- 361 Dosovitskiy, Alexey, Lucas Beyer, Alexander Kolesnikov, Dirk Weissenborn, Xiaohua
362 Zhai, Thomas Unterthiner, Mostafa Dehghani, Matthias Minderer, Georg Heigold,

- 363 Sylvain Gelly, Jakob Uszkoreit, and Neil Houlsby (June 2021). *An Image is Worth*
364 *16x16 Words: Transformers for Image Recognition at Scale*. arXiv:2010.11929 [cs].
365 DOI: 10.48550/arXiv.2010.11929.
- 366 Gawlikowski, Jakob, Cedrique Rovile Njjeutcheu Tassi, Mohsin Ali, Jongseok Lee, Matthias
367 Humt, Jianxiang Feng, Anna Kruspe, Rudolph Triebel, Peter Jung, Ribana Roscher,
368 et al. (2023). “A survey of uncertainty in deep neural networks”. In: *Artificial Intel-*
369 *ligence Review*, pp. 1–77.
- 370 Gimenez, Olivier, Maëlis Kervellec, Jean-Baptiste Fanjul, Anna Chainé, Lucile Marescot,
371 Yoann Bollet, and Christophe Duchamp (Apr. 2022). “Trade-off between deep learn-
- 372 ing for species identification and inference about predator-prey co-occurrence”. en.
373 In: *Computo*. ISSN: 2824-7795. DOI: 10.57750/yfm2-5f45.
- 374 Guo, Chuan, Geoff Pleiss, Yu Sun, and Kilian Q. Weinberger (Aug. 2017). *On Calibration*
375 *of Modern Neural Networks*. arXiv:1706.04599 [cs].
- 376 Howard, Andrew, Mark Sandler, Grace Chu, Liang-Chieh Chen, Bo Chen, Mingxing
377 Tan, Weijun Wang, Yukun Zhu, Ruoming Pang, Vijay Vasudevan, Quoc V. Le, and
378 Hartwig Adam (Nov. 2019). *Searching for MobileNetV3*. arXiv:1905.02244 [cs].
- 379 Jung, Alexander B., Kentaro Wada, Jon Crall, Satoshi Tanaka, Jake Graving, Christoph
380 Reinders, Sarthak Yadav, Joy Banerjee, Gábor Vecsei, Adam Kraft, Zheng Rui, Jirka
381 Borovec, Christian Vallentin, Semen Zhydenko, Kilian Pfeiffer, Ben Cook, Ismael
382 Fernández, François-Michel De Rainville, Chi-Hung Weng, Abner Ayala-Acevedo,
383 Raphael Meudec, Matias Laporte, et al. (2020). *imgaug*. [https://github.com/](https://github.com/aleju/imgaug)
384 [aleju/imgaug](https://github.com/aleju/imgaug). Online; accessed 01-Feb-2020.
- 385 Liu, Ze, Han Hu, Yutong Lin, Zhuliang Yao, Zhenda Xie, Yixuan Wei, Jia Ning, Yue Cao,
386 Zheng Zhang, Li Dong, Furu Wei, and Baining Guo (Apr. 2022). *Swin Transformer*
387 *V2: Scaling Up Capacity and Resolution*. arXiv:2111.09883 [cs].

- 388 Liu, Zhuang, Hanzi Mao, Chao-Yuan Wu, Christoph Feichtenhofer, Trevor Darrell, and
389 Saining Xie (Mar. 2022). *A ConvNet for the 2020s*. arXiv:2201.03545 [cs]. DOI: 10.
390 48550/arXiv.2201.03545.
- 391 Maher, Mohamed and Meelis Kull (Oct. 2021). *Instance-based Label Smoothing For Bet-*
392 *ter Calibrated Classification Networks*. arXiv:2110.05355 [cs].
- 393 Minderer, Matthias, Josip Djolonga, Rob Romijnders, Frances Hubis, Xiaohua Zhai,
394 Neil Houlsby, Dustin Tran, and Mario Lucic (Oct. 2021). *Revisiting the Calibration*
395 *of Modern Neural Networks*. arXiv:2106.07998 [cs].
- 396 Mitterwallner, Veronika, Anne Peters, Hendrik Edelhoff, Gregor Mathes, Hien Nguyen,
397 Wibke Peters, Marco Heurich, and Manuel J. Steinbauer (2023). “Automated visitor
398 and wildlife monitoring with camera traps and machine learning”. In: *Remote Sensing*
399 *in Ecology and Conservation* n/a.n/a. DOI: <https://doi.org/10.1002/rse2.367>.
400 eprint: [https://zslpublications.onlinelibrary.wiley.com/doi/pdf/10.](https://zslpublications.onlinelibrary.wiley.com/doi/pdf/10.1002/rse2.367)
401 [1002/rse2.367](https://zslpublications.onlinelibrary.wiley.com/doi/pdf/10.1002/rse2.367).
- 402 Nair, Tanya, Doina Precup, Douglas L. Arnold, and Tal Arbel (Oct. 2018). *Exploring*
403 *Uncertainty Measures in Deep Networks for Multiple Sclerosis Lesion Detection and*
404 *Segmentation*. arXiv:1808.01200 [cs]. DOI: 10.48550/arXiv.1808.01200.
- 405 Norman, Danielle L., Philipp H. Bischoff, Oliver R. Wearn, Robert M. Ewers, J. Marcus
406 Rowcliffe, Benjamin Evans, Sarab Sethi, Philip M. Chapman, and Robin Freeman
407 (2023). “Can CNN-based species classification generalise across variation in habi-
408 tat within a camera trap survey?” en. In: *Methods in Ecology and Evolution* 14.1.
409 eprint: <https://onlinelibrary.wiley.com/doi/pdf/10.1111/2041-210X.14031>, pp. 242–
410 251. ISSN: 2041-210X. DOI: 10.1111/2041-210X.14031.
- 411 Norouzzadeh, Mohammad Sadegh, Anh Nguyen, Margaret Kosmala, Alexandra Swan-
412 son, Meredith S. Palmer, Craig Packer, and Jeff Clune (June 2018). “Automatically
413 identifying, counting, and describing wild animals in camera-trap images with deep

- 414 learning”. en. In: *Proceedings of the National Academy of Sciences* 115.25. ISSN:
415 0027-8424, 1091-6490. DOI: 10.1073/pnas.1719367115.
- 416 Parsons, Arielle W., Kenneth F. Kellner, Christopher T. Rota, Stephanie G. Schuttler,
417 Joshua J. Millspaugh, and Roland W. Kays (2022). “The effect of urbanization on
418 spatiotemporal interactions between gray foxes and coyotes”. en. In: *Ecosphere* 13.3.
419 eprint: <https://onlinelibrary.wiley.com/doi/pdf/10.1002/ecs2.3993>, e3993. ISSN: 2150-
420 8925. DOI: 10.1002/ecs2.3993.
- 421 Platt, John (June 2000). “Probabilistic Outputs for Support Vector Machines and Com-
422 parisons to Regularized Likelihood Methods”. In: *Adv. Large Margin Classif.* 10.
- 423 Rahaman, Rahul and Alexandre H. Thiery (Nov. 2021). *Uncertainty Quantification and*
424 *Deep Ensembles*. arXiv:2007.08792 [cs, stat].
- 425 Ridnik, Tal, Emanuel Ben-Baruch, Asaf Noy, and Lihi Zelnik-Manor (Aug. 2021). *ImageNet-*
426 *21K Pretraining for the Masses*. arXiv:2104.10972 [cs]. DOI: 10.48550/arXiv.2104.
427 10972.
- 428 Rigoudy, Noa, Gaspard Dussert, Abdelbaki Benyoub, Aurélien Besnard, Carole Birck,
429 Jérôme Boyer, Yoann Bollet, Yoann Bunz, Gérard Caussimont, Elias Chetouane,
430 Jules Chiffard Carriburu, Pierre Cornette, Anne Delestrade, Nina De Backer, Lucie
431 Dispan, Maden Le Barh, Jeanne Duhayer, Jean-François Elder, Jean-Baptiste Fan-
432 jul, Jocelyn Fonderflick, Nicolas Froustey, Mathieu Garel, William Gaudry, Agathe
433 Gérard, Olivier Gimenez, Arzhela Hemery, Audrey Hemon, Jean-Michel Jullien,
434 Daniel Knitter, Isabelle Malafosse, Mircea Marginean, Louise Ménard, Alice Ou-
435 vrier, Gwennaelle Pariset, Vincent Prunet, Julien Rabault, Malory Randon, Yann
436 Raulet, Antoine Régnier, Romain Ribière, Jean-Claude Ricci, Sandrine Ruetter, Yann
437 Schneylin, Jérôme Sentilles, Nathalie Siefert, Bethany Smith, Guillaume Terpereau,
438 Pierrick Touchet, Wilfried Thuiller, Antonio Uzal, Valentin Vautrain, Ruppert Vi-
439 mal, Julian Weber, Bruno Spataro, Vincent Miele, and Simon Chamaillé-Jammes
440 (Oct. 2023). “The DeepFaune initiative: a collaborative effort towards the automatic

- 441 identification of European fauna in camera trap images”. In: *European Journal of*
442 *Wildlife Research* 69.6, p. 113. DOI: 10.1007/s10344-023-01742-7.
- 443 Simpson, Robert, Kevin R. Page, and David De Roure (Apr. 2014). “Zooniverse: ob-
444 serving the world’s largest citizen science platform”. en. In: *Proceedings of the 23rd*
445 *International Conference on World Wide Web*. Seoul Korea: ACM, pp. 1049–1054.
446 ISBN: 978-1-4503-2745-9. DOI: 10.1145/2567948.2579215.
- 447 Sollmann, Rahel (2018). “A gentle introduction to camera-trap data analysis”. en. In:
448 *African Journal of Ecology* 56.4. eprint: <https://onlinelibrary.wiley.com/doi/pdf/10.1111/aje.12557>,
449 pp. 740–749. ISSN: 1365-2028. DOI: 10.1111/aje.12557.
- 450 Szegedy, Christian, Vincent Vanhoucke, Sergey Ioffe, Jonathon Shlens, and Zbigniew
451 Wojna (Dec. 2015). *Rethinking the Inception Architecture for Computer Vision*.
452 arXiv:1512.00567 [cs].
- 453 Tan, Mingxing and Quoc V. Le (June 2021). *EfficientNetV2: Smaller Models and Faster*
454 *Training*. arXiv:2104.00298 [cs].
- 455 Wang, Deng-Bao, Lanqing Li, Peilin Zhao, Pheng-Ann Heng, and Min-Ling Zhang
456 (2023). “On the Pitfall of Mixup for Uncertainty Calibration”. en. In: pp. 7609–
457 7618.
- 458 Whytock, Robin C., Thijs Suijten, Tim van Deursen, Jędrzej Świeżewski, Hervé Mer-
459 miaghe, Nazaire Madamba, Narcisse Mouckoumou, Joeri A. Zwerts, Aurélie Flore
460 Koumba Pambo, Laila Bahaa-el-din, Stephanie Brittain, Anabelle W. Cardoso, Philipp
461 Henschel, David Lehmann, Brice Roxan Momboua, Loïc Makaga, Christopher Or-
462 bell, Lee J. T. White, Donald Midoko Iponga, and Katharine A. Abernethy (2023).
463 “Real-time alerts from AI-enabled camera traps using the Iridium satellite network: A
464 case-study in Gabon, Central Africa”. en. In: *Methods in Ecology and Evolution* 14.3.
465 eprint: <https://onlinelibrary.wiley.com/doi/pdf/10.1111/2041-210X.14036>, pp. 867–
466 874. ISSN: 2041-210X. DOI: 10.1111/2041-210X.14036.

- 467 Whytock, Robin C., Jędrzej Świeżewski, Joeri A. Zwerts, Tadeusz Bara-Ślupski, Aurélie
468 Flore Koumba Pambo, Marek Rogala, Laila Bahaa-el-din, Kelly Boekee, Stephanie
469 Brittain, Anabelle W. Cardoso, Philipp Henschel, David Lehmann, Brice Momboua,
470 Cisquet Kiebou Opepa, Christopher Orbell, Ross T. Pitman, Hugh S. Robinson, and
471 Katharine A. Abernethy (2021). “Robust ecological analysis of camera trap data la-
472 belled by a machine learning model”. en. In: *Methods in Ecology and Evolution* 12.6.
473 _eprint: <https://onlinelibrary.wiley.com/doi/pdf/10.1111/2041-210X.13576>, pp. 1080–
474 1092. ISSN: 2041-210X. DOI: 10.1111/2041-210X.13576.
- 475 Wightman, Ross (2019). *PyTorch Image Models*. [https://github.com/rwightman/
476 pytorch-image-models](https://github.com/rwightman/pytorch-image-models). DOI: 10.5281/zenodo.4414861.
- 477 Willi, Marco, Ross T. Pitman, Anabelle W. Cardoso, Christina Locke, Alexandra Swan-
478 son, Amy Boyer, Marten Veldthuis, and Lucy Fortson (2019). “Identifying animal
479 species in camera trap images using deep learning and citizen science”. en. In: *Meth-
480 ods in Ecology and Evolution* 10.1. _eprint: [https://onlinelibrary.wiley.com/doi/pdf/10.1111/2041-
210X.13099](https://onlinelibrary.wiley.com/doi/pdf/10.1111/2041-
481 210X.13099), pp. 80–91. ISSN: 2041-210X. DOI: 10.1111/2041-210X.13099.
- 482 Wu, Xixin and Mark Gales (Jan. 2021). *Should Ensemble Members Be Calibrated?*
483 arXiv:2101.05397 [cs, stat].
- 484 Zhang, Hongyi, Moustapha Cisse, Yann N. Dauphin, and David Lopez-Paz (Apr. 2018).
485 *mixup: Beyond Empirical Risk Minimization*. arXiv:1710.09412 [cs, stat]. DOI: 10.
486 48550/arXiv.1710.09412.
- 487 Zuleger, Annika, Andrea Perino, Florian Wolf, Helen C. Wheeler, and Henrique M.
488 Pereira (2023). “Long-term monitoring of mammal communities in the Peneda-Gerês
489 National Park using camera trap data”. In: *ARPHA Preprints* 4, ARPHA Preprints.
490 DOI: 10.3897/arphapreprints.e99983. eprint: [https://doi.org/10.3897/
arphapreprints.e99983](https://doi.org/10.3897/
491 arphapreprints.e99983).

492 Supplementary materials

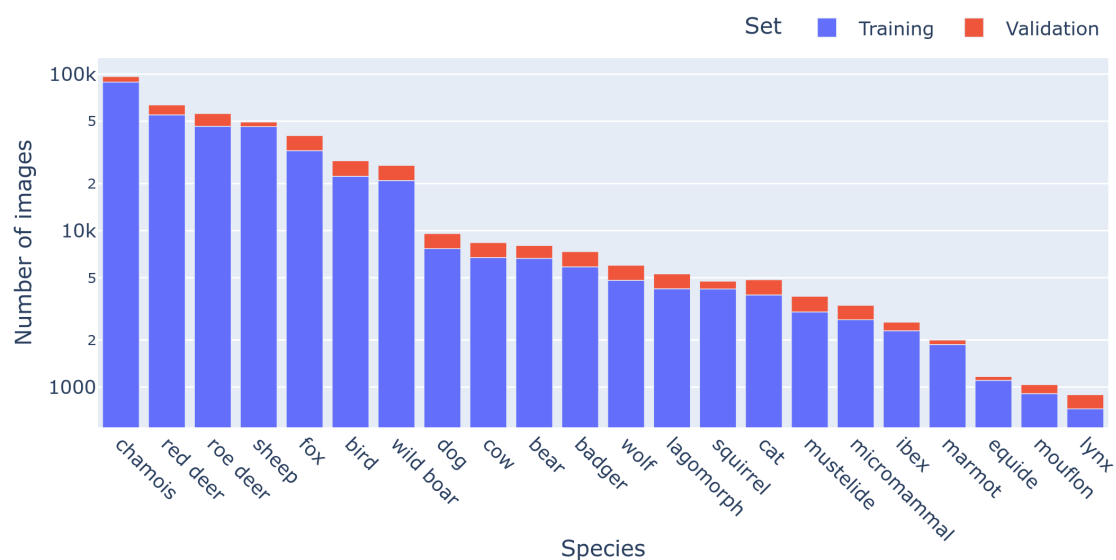


Figure 6: Number of images in the training and validation sets, for each species. Log scale is used to improve the readability of the rarer classes.

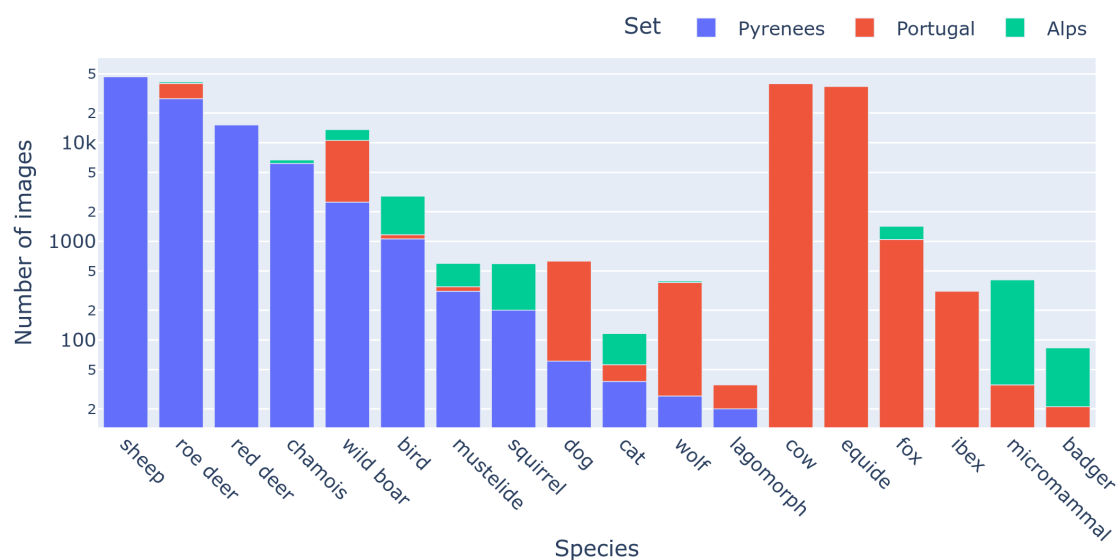


Figure 7: Number of images in the three out-of-sample datasets, for each species. Log scale is used to improve the readability of the rarer classes.

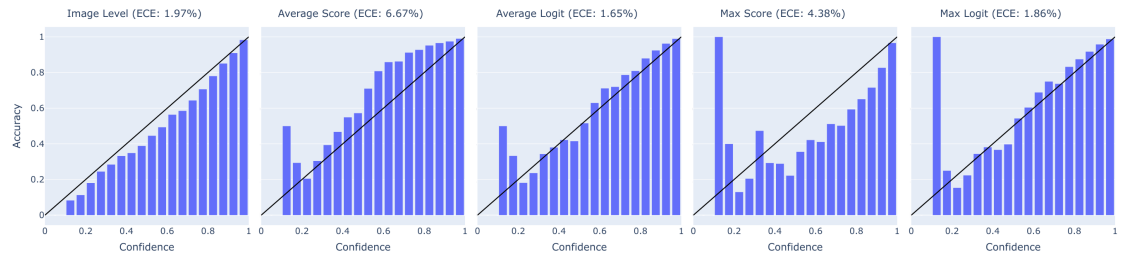


Figure 8: Reliability histogram of the ConvNext model, using the 3 test sets pooled together, and without temperature scaling.